A 3-D Deformable Surface Method for Automatic Hippocampus-Amygdala Complex Segmentation

M. M. Karimi [1], N. Batmanghelich [1,2], H. Soltanian-Zadeh [1,2,3], C. Lucas [1,2]
[1] University of Tehran, Tehran, Iran, [2] Institute for Studies in Theoretical Physics and Mathematics, Tehran, Iran,
[3] Henry Ford Health System, Detroit, Michigan, United states

Abstract—**In this paper, we propose an atlas-based method for hippocampus-amygdala complex segmentation. An atlas was registered on all subjects and its transformation was calculated for each subject. This transformation was applied to the structural segmentation of the complex obtained from atlas to construct an initial surface for the hippocampus-amygdala complex of each subject. A possibility approach was introduced for the segmentation process. Two different kinds of deformation based on edges and information obtained from tissue segmentation have been used to find different parts of the complex. A new energy was defined to use tissue information. This energy is adopted to expand the model to embed more dominant gray matter points in the volume and also withdraws from dominant white matter and CSF points. The initial shape was divided into several parts. In the normal direction of the center of each part, we constructed a profile which searched for the best point which maximized this new energy. This algorithm is reliable for finding the overall shape of the complex. It overcomes the poor features of the complex such as weak edges and noise. The algorithm was examined on 5 different subjects and validated using two different validation methods.**

Keywords—**brain segmentation, deformable surface, amygdale, hippocampus**

I. Introduction

The amygdala is an almond-shaped structure, which is situated anterior and partly superior to the tip of temporal horn of the lateral ventricle [1]. The hippocampus is a cylindrical structure, voluminous interiorly, extending as much as 4-5 cm from the tip of the temporal horn to the splenium of the carpuscallosum where it becomes continuous with the fornix. The hippocampus commonly is divided into three parts: head, body, and tail [2].

In the coronal view of brain images the boundary between hippocampus and amygdale is often indistinct. In fact, amygdale and hippocampus were separated just with the landmarks of temporal horn of lateral ventricle. These landmarks usually are so vague and tolerable that even for an expert, it is impossible to say where the exact boundary between amygdale and hippocampus is. However, this boundary may be seen more clearly in sagittal views. One way to distinguish these two structures is to segment these structures in sagittal slices from each other and then cut the volume is coronal view. The points obtained from previous stage of segmentation in sagittal view appear in the coronal view and make the boundary between amygdala and hippocampus [1]. Because the boundry between amygdala and hippocampus was not apparent in our data set, we decided to segment the whole complex of these structures altogether.

We used a deformable surface for this purpose. A powerful method for finding an object in a 3D image is deformable surface [3], [4]. This surface usually moves towards the desired object with information extracted from geometrical features (internal forces) and information obtained from edges and grayscales of an image (external forces) [3]. But when an image includes noise or weak edges, such as hippocampus-amygdala complex, the model should move toward the target passing weak edges and partial volumes [5].

We propose a method to solve this problem using information obtained from the tissue segmentation. We introduce three kinds of deformation that each one has a kind of effect in the deformation process.

II. Methodology

The basis of the simplex meshes model was used as the basis of our model. The simplex meshes model is a 3-D deformable surface. At the first, it was used as a representation [6] model but after that Delingette. et al used it for segmentation purposes.

As seen in Fig.1 each vertex of the simplex mesh has only three neighbors. We used this model because the calculation of the normal vector and curvature is straight-forward and can be extracted from any triangulation algorithm using duality property between simplex meshes and triangulation [7].

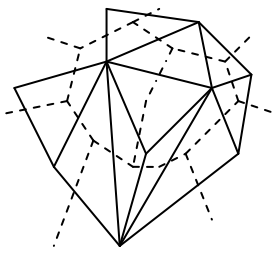

Fig. 1. Duality between triangulation and simplex meshes. Solid lines are lines of triangulation.

As mentioned before in this model each vertex is connected to three neighbors. The normal vector at each vertex is computed as:

$$\mathbf{n}_i = \frac{\mathbf{P}_{N_1(i)} \times \mathbf{P}_{N_2(i)} + \mathbf{P}_{N_2(i)} \times \mathbf{P}_{N_3(i)} + \mathbf{P}_{N_3(i)} \times \mathbf{P}_{N_1(i)}}{\left\| \mathbf{P}_{N_1(i)} \times \mathbf{P}_{N_2(i)} + \mathbf{P}_{N_2(i)} \times \mathbf{P}_{N_2(i)} + \mathbf{P}_{N_2(i)} \times \mathbf{P}_{N_3(i)} \right\|} \quad (1)$$

As seen in Fig.2, The positions of the three neighbors of i-th vertex are shown by $\mathbf{P}_{N_1(i)}, \mathbf{P}_{N_2(i)}, \mathbf{P}_{N_3(i)}$.

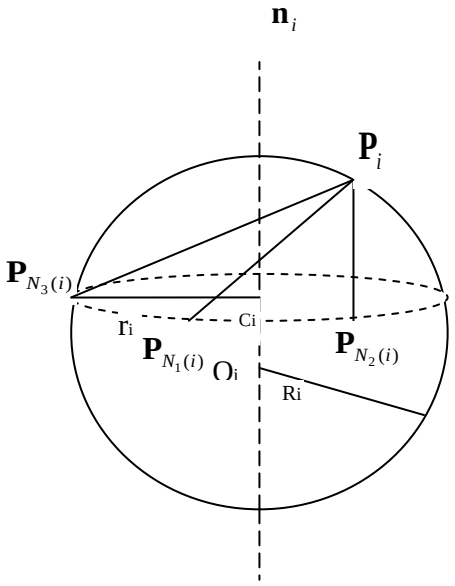

Fig. 2. A typical vertex with its three neighbors.

The segmentation process is divided to these steps:

1) Initialization: This is the first step of the deformation that has fundamental rule in deformation process. In this step, a deformable surface is put near the hippocampus-amygdala complex. The more adjacent to the border, the better segmentation result. An atlas-based method was used for this purpose. We used SPM (statistical parametric mapping) toolbox [8] as a registration tool and projected a structural segmentation of the complex on the subjects' MRI. This used an affine transform obtained from the atlas registration to these subjects. Because we did not use nonlinear transformations, in some parts of the initial complex, the model deviated greatly from the desired structure. Thus, an erosion algorithm was done on the initial shape on each slice to close this shape to a region of interest and then we constructed the initial surfaces.
2) Initial model: After initialization, isosurface algorithm was exerted on the initial shape and triangulation model of the surface was extracted.
3) Simplex meshes model: From duality property between simplex meshes and triangulation [7], vertices and faces of simplex meshes were extracted (see Fig. 1).
4) Deformation: After constructed, the model must deform. Three kinds of deformation are proposed:
   A) Deformation based on a new gradient based force that pulls different parts of the model with its related vertices to the desired edges. This force is defined as:

$$\mathbf{F}_i = \sum_{j=1}^{J} u_{ij} (\mathbf{F}_{ex,j} \cdot \mathbf{n}_j)\ \mathbf{n}_j \quad (2)$$

where j depicts the cluster or part number and i is the vertex number. For each cluster, we found the center of the cluster ($\mathbf{S}_j$) and the normal vector was computed at the center of each cluster ($\mathbf{n}_j$). For each vertex, a fuzzy membership function was introduced which determined the membership of each vertex to each cluster (u_{ij}). We used Euclidean distance ($d(\mathbf{P}_i, \mathbf{S}_j)$) for the definition of u_{ij}:

$$u_{ij} = \frac{1}{1 + d(\mathbf{P}_i, \mathbf{S}_j)} \quad (3)$$

The position of vertex i is represented by $\mathbf{P}_i$ and $\mathbf{F}_{ex,j}$ is an external force which is defined in [3] and is enforced to the center of the j-th cluster:

$$\mathbf{F}_{ex,j} = \nabla^2 (I(x_j, y_j, z_j) * G_\sigma) \quad (4)$$

No internal forces are defined in this kind of deformation because the curvature continuity constraint will be satisfied with this special kind of deformation. One vertex moves mostly in the direction of the normal vector of the part that this vertex has the most membership to it. It makes different parts of the model move smoothly. For each vertex we have:

$$\mathbf{P}_i^{t+1} = \mathbf{P}_i^t + \beta \cdot \mathbf{F}_i \quad (5)$$

where $\mathbf{P}_i^{t+1}$ is the position of the i-th vertex in t+1 iteration and β is the factor that determines the rate of deformation.

B) The second kind of deformation is based on tissue segmentation. With FSL (FMRIB Software Library) software [9]

each brain was divided into 3 separate volumes of gray matter, white matter and CSF. In each part of the model which must deform with this method, a profile is constructed at the position of the vertex that is representative of that part. This profile is constructed in the normal direction of this vertex and has 7 points. We search in the direction of this profile to find the point that maximizes this energy function:

$$E = \sum_{i=1}^{N} (GM_i - WM_i - CSF_i) \qquad (6)$$

This energy is adopted to expand the model to embed more dominant gray matter points to the volume and also withdraws from dominant white matter and CSF points. N is the number of points embedded by the deformable surface. In the direction of each profile, we change the position of the center of each part. The position of the vertices changes according to the following equation:

$$\mathbf{P}_{i,k}^{t+1} = \mathbf{P}_{i,k}^{t} + u_{ij} \cdot (k-4) \cdot \mathbf{n}_j \qquad (7)$$
$$k = 1,2,...,7$$

where $\mathbf{P}_{i,k}^{t}$ is the position of the i-th vertex when the center of the j-th cluster or part moves to the k-th point of its normal profile. After each step of the search, we find the energy defined in equation (6) and is related to move the center of the j-th part to k-th point of its profile. In each step of search on this profile, some points may add or subtract from the points embedded by the surface and N may change. If a part of the model is in a CSF or white matter dominant region, the model tries to increase energy by going to the point at the profile that eliminate these points and if it is in the gray matter dominant region, it will be expanded to embed more dominant gray matter points. The point which has the maximum energy among these 7 points is selected as target point and the model deforms to this point. To avoid the redundant calculation we used a threshold value for membership function. It means that if u_{ij} is lower than a threshold value, we won't move its related vertex position at all.

It causes the model to deform only in the vicinity of the j-th part.

C) After reaching to the vicinity of the complex border, the model moves to the border precisely and will find the details of the border. This step is done similar to the previous deformable models. We used internal forces and external forces which are defined in the [3].

5) From duality property between simplex meshes and triangulation [7], vertices and faces of the triangulation model were extracted. We did this process because we needed to visualize the surface as a triangulation model and we didn't access to the simplex meshes viewer.

6) We used two criteria for validation of the results. One of them was the measurement of the percent of intersection between this method of segmentation and manual segmentation. The Tanimoto measure between two sets **X** and **Y** is defined as:

$$\frac{{}^{n}X \cap Y}{{}^{n}X + {}^{n}Y - {}^{n}X \cap Y} = \frac{{}^{n}X \cap Y}{{}^{n}X \cup Y} \qquad (8)$$

Because we had the manual segmentation of this complex in each slice separately, we had to cut the final surface after deformation in each slice, but some vertices put between two slices in the final surface. If we wanted to give these vertices to the slice that is more adjacent to these vertices, in another slice might cause discontinuity. Consequently, we defined another volume which had a value that determined each voxel has how much membership in the final segmentation. The woxels which put into the surface had the value of 1. But the voxels which put in the vicinity of the border may have any value between 0 and 1 according to the Euclidean distance to the nearest vertices of the model. When we want to calculate the number of voxels which intersect to the manual segmentation, the voxels in the border are counted with their value between 0 and 1.

Another criterion used specially for this complex segmentation was the percent of gray matter which put into the surface. Because we used fuzzy tissue segmentation, each voxel in the gray matter volume has a membership between 0 and 1. We added the membership of the vexels which put into the surface (GM_{int}) and divided it to the numbers of these points (N). We called it possibility factor (P.F).

$$P.F = \frac{\sum GM_{\text{int}}}{N} \qquad (9)$$

III. Results

We implemented this method on volume MRI images of 5 subjects whose manual expert segmentation of hippocampus were also available. This data was obtained from Internet Brain Segmentation Repository (IBSR). Because in some parts of the complex we have weak edges when the complex deforms just with the forces which are defined based on gradient, it's trapped to these weak edges and can't reach to the strong edges. After 3-D structural projection of complex to each subject, in each slice that we had this complex, this part of complex was divided to 8 parts (see Fig.3). In the superior parts and parts which are adjacent to the medial and lateral parts of the image, we have partial volumes which produce several layers of weak edges. If initial shape is far a way from strong edges, it will be trapped to these weak edges. In the inferior parts of the complex, we have a thin layer of white matter that can be detected with gradient based external forces. We found adjacent vertices of deformable surface to the representative of each part. At the inferior parts of the surface, the vertices deform with equation (5) but at the other parts, they deform with equation (7). Finally, a final tuning was exerted on all vertices. The result of deformation is shown in Fig. 4. For validation of the method, we used two criteria. First, we found the percent of intersection between manual segmentation and segmentation using this method. But we also validated our method with a possibility factor which is related to this complex specially. Because we knew that this complex is constructed by gray matter, we computed the average of gray matter of all voxels embedded by deformable surface. Table1 shows the results of this method for right Hippocampus-Amygdala complex segmentation of 5 subjects.

Fig. 3. Intersection of 3-D deformable surface with one slice. Each slice is divided to 8 parts and after that the nearest vertex of the deformable surface is selected as the center of this part.

IV. Discussion

In this paper, we proposed a knowledge-based deformable surface which moves toward target with a multi approach of deformation depending on the parts that move. We divided this model to separate parts and these parts with their adjacent vertices move toward the desired object. After reaching to the vicinity of the object, we did final tuning on the model. This model has some advantages and disadvantages. Its advantage is that because it uses tissue and edges information simultaneously, it can make a reliable decision. The results also confirm this claim. But its disadvantage is that it can not be extended to the other structures because this method is designed only for this structure and purpose. It is not generic. The other disadvantage of this method is the time consuming and boring computation especially with PC. Because the algorithm must check any changes that occur in the energy function related to the changes of the points of the model, it takes much time to be done this computation by PC. In the future works, we will follow an approach to separate hippocampus and amygdala from each other and also introduce a method to optimize the computational aspects of the algorithm.

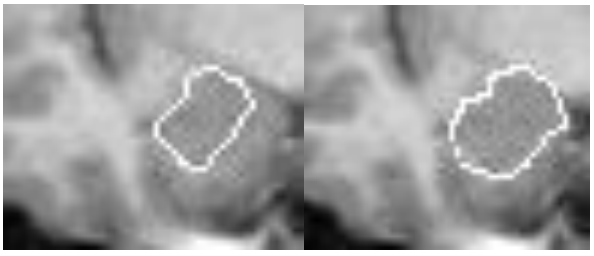

(a) (b)

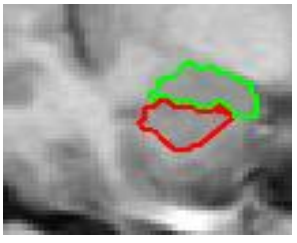

(c)

Fig. 3. Deformation process on slice 61. (a) initial contour after registration (b) final cut of the surface after deformation. (c) manual expert segmentation. The red contour is hippocampus and green contour is amygdala.

TABLE I
Possibility factor and percent of intersection between manual and automatic segmentations.

Subjects	1	2	3	4	5
Possibility factor	0.84	0.82	0.82	0.83	0.82
Percent of intersection	85	87	82	78	80

REFERENCES

[1] A. Convit, P. McHugh, O. T. Wolf, M. J. Leon, M. Bobinski, S. Desanti, A. Roche, W. Tsui, "MRI volum of the amygdale: a reliable method allowing separation from the hippocampal formation," *Psychiatry Research: Neuroimaging Section* , vol. 90, pp. 113-123, 1999.

[2] J. C. Tamraz, Y. G. Comair, Atlas of Regional Anatomy of the Brain Using MRI. Berlin: Springer, 2000.

[3] A. Ghanei, H. Soltanian-Zadeh, "A Discrete Curvature-Based Deformable Surface Model with Application to Segmentation of Volumetric Image*," IEEE transaction on information technology in biomedicine*, vol. 6, no. 4, pp. 285-296, December 2002.

[4] H. Delingette, "General object reconstruction based on simplex meshes," *International Jornal of Computer Vision 32*, vol. 1, pp.111-146, 1998.

[5] D. Shen, C. Davatzikos, "A hierarchical Deformable Model Using Statistical and Geometric Information," *IEEE Workshop on Mathematical Methods in Biomdeical Image Analysis (MMBIA2000),* pp. 1-10, South Carolina, 2000.

[6] H. Delingette, "Simplex Meshes: a General Representation for 3D Shape Reconstruction," *Technical Report 2214*, pp.1-70, INRIA, MARCH 1994.

[7] A. Pitiot, H. Delingette, N. Ayache, P. M. Thompson, "Expert Knowledge Guided Segmentation System for Brain MRI," *Medical Image Computing and Computer-Assisted intervention MICCAI'03,* vol. 2879, pp. 644-652, November 2003.

[8] http://www.fil.ion.ucl.ac.uk/spm/

[9] http://www.fmrib.ox.ac.uk/fsl/